UC San Diego
UC San Diego Previously Published Works

Title

Hexa (ethylene glycol) derivative of benzothiazole aniline promotes dendritic spine formation through the RasGRF1–Ras dependent pathway

Permalink

https://escholarship.org/uc/item/64j6d12z

Journal

Biochimica et Biophysica Acta, 1862(2)

ISSN

0006-3002

Authors

Lee, Nathanael J
Song, Jung Min
Cho, Hyun-Ji
et al.

Publication Date

2016-02-01

DOI

10.1016/j.bbadis.2015.12.007

Peer reviewed

CrossMark

Hexa (ethylene glycol) derivative of benzothiazole aniline promotes dendritic spine formation through the RasGRF1–Ras dependent pathway☆,☆☆

Nathanael J. Lee [a,1], Jung Min Song [a,1], Hyun-Ji Cho [d,1], You Me Sung [a,b,1], Taehee Lee [a], Andrew Chung [a], Sung-Ha Hong [a,b], Jessica L. Cifelli [e], Mark Rubinshtein [e], Lila K. Habib [f], Christina C. Capule [e], R. Scott Turner [b], Daniel T.S. Pak [c], Jerry Yang [e], Hyang-Sook Hoe [a,b,d,*]

[a] Department of Neuroscience, Georgetown University Medical Center, Washington, DC 20057, USA
[b] Department of Neurology, Georgetown University Medical Center, Washington, DC 20057, USA
[c] Department of Pharmacology, Georgetown University Medical Center, Washington, DC 20057, USA
[d] Department of Neural Development and Disease, Korea Brain Research Institute (KBRI), Cheomdan-ro, Dong-gu, Daegu 701-300, Republic of Korea
[e] Department of Chemistry and Biochemistry, University of California, San Diego, La Jolla, CA 92093, USA
[f] Department of Bioengineering, University of California, San Diego, La Jolla, CA 92093, USA

ARTICLE INFO

ABSTRACT

Our recent study demonstrated that an amyloid-β binding molecule, BTA-EG4, increases dendritic spine number via Ras-mediated signaling. To potentially optimize the potency of the BTA compounds, we synthesized and evaluated an amyloid-β binding analog of BTA-EG4 with increased solubility in aqueous solution, BTA-EG6. We initially examined the effects of BTA-EG6 on dendritic spine formation and found that BTA-EG6-treated primary hippocampal neurons had significantly increased dendritic spine number compared to control treatment. In addition, BTA-EG6 significantly increased the surface level of AMPA receptors. Upon investigation into the molecular mechanism by which BTA-EG6 promotes dendritic spine formation, we found that BTA-EG6 may exert its effects on spinogenesis via RasGRF1-ERK signaling, with potential involvement of other spinogenesis-related proteins such as Cdc42 and CDK5. Taken together, our data suggest that BTA-EG6 boosts spine and synapse number, which may have a beneficial effect of enhancing neuronal and synaptic function in the normal healthy brain.

© 2015 Elsevier B.V. All rights reserved.

1. Introduction

Alzheimer's Disease (AD) is a progressive neurodegenerative disease, characterized by deposition of amyloid-β (Aβ) plaques and neurofibrillary tangles of Tau protein [1–3]. Several recent studies have demonstrated that Aβ plaques decrease dendritic spine density and synapse number as well as impair learning and memory [4–6]. Interestingly, Tau also affects dendritic spine number [7,8]. For instance, the acceleration of Tau pathology results in the synaptic and neuronal loss in a transgenic (Tg) mouse model of AD. Additionally, the overexpression of Tau has been shown to increase spine density, whereas Tau mutants have reduced dendritic spine density [9]. Therefore, either blocking/neutralizing Aβ toxicity or enhancing the expression of Tau may be potential therapeutic targets for AD by enhancing synaptic function.

Our previous studies have shown that a member of the benzothiazole aniline (BTA) class of compounds, specifically BTA-EG4, affects normal synaptic function by increasing dendritic spine number through Ras-dependent mechanisms [10]. Additionally, we found that BTA-EG4 ameliorates dendritic spine formation deficits in 3xTg AD mice 2 weeks after injection and increases Ras activity [11].

In the present study, we examined another BTA analog that can bind to Aβ [12–14], BTA-EG6, containing a hexa (ethylene glycol) water-solubilizing group to enhance solubility in aqueous solutions compared to BTA-EG4. We initially examined whether BTA-EG6 can affect dendritic spine formation and synaptic function in vitro. We found that BTA-EG6 significantly increased dendritic spine number, as well as puncta numbers of synaptophysin and postsynaptic (PSD)-95.
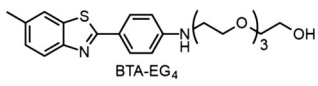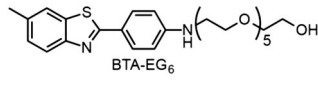
Table 1
Solubility comparison of BTA-EG6 and BTA-EG4 in PBS (pH 7.4).

Compound	MW (g/mol)	μg/ml	Solubility, S (M)	logS
BTA-EG$_4$	416.54	7.0 ± 0.5	0.000017 ± 0.000001	-4.78 ± 0.07
BTA-EG$_6$	504.64	1247 ± 161	0.002470 ± 0.000319	-2.61 ± 0.11

In addition, we found that BTA-EG6 significantly increased the cell surface levels of GluA1 and GluA2. BTA-EG6 was able to alter the levels of Ras signaling proteins, including Ras guanine nucleotide releasing factor1 (RasGRF1), extracellular signal-regulated kinase (ERK), and cAMP responsive element binding protein (CREB). Also, we found that the transfection with RasGRF1 shRNA and RasN17 (inactive Ras mutant) inhibited the effects of BTA-EG6 on dendritic spine formation. Moreover, we found that BTA-EG6 increased the puncta number of calcium/calmodulin-dependent protein kinase II α (CaMKIIα), but not CaMKIIβ. However, BTA-EG6 did not alter the levels of Rap signaling proteins, which are implicated in dendritic spine retardation. Taken together, these results suggest that BTA-EG6 affects dendritic spine formation in vitro in a Ras- but not Rap-dependent manner.

2. Materials and methods

2.1. Synthesis of BTA-EG6

BTA-EG6 was prepared as previously described [13,15,16]. Briefly, a flame-dried flask was charged with 1-Iodo-3,6,9,12,15-pentaoxaheptadecanol (0.18 g, 0.45 mmol), 2-(p-aminophenyl)-6-methyl-benzothiazole (0.09 g, 0.38 mmol), and potassium carbonate (0.39 g, 2.8 mmol) in dry acetone (4 mL) under reflux conditions for 3 days. The acetone was removed and the residue was taken up into dichloromethane, and separated from an insoluble precipitate (presumably excess potassium carbonate and potassium iodide). After the precipitate was removed by filtration, the solution was washed
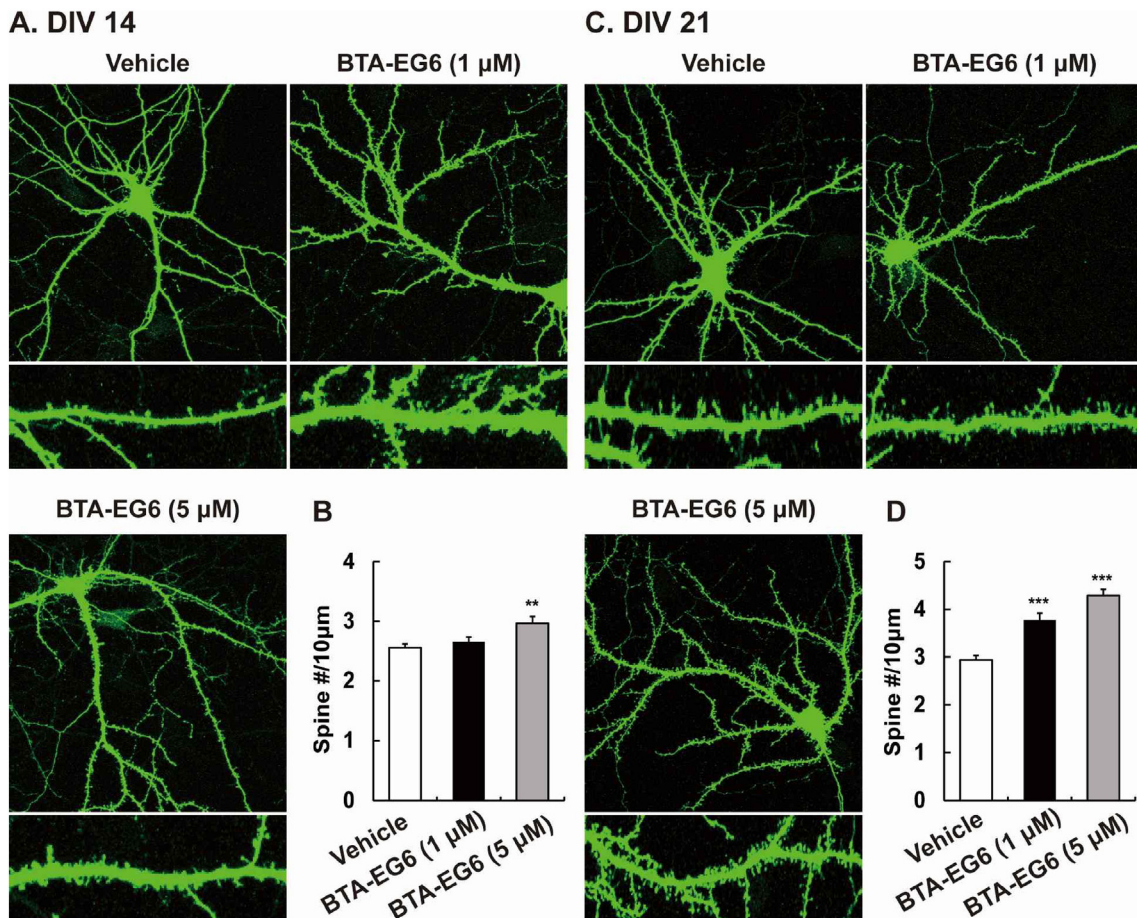

Fig. 1. BTA-EG6 increases dendritic spine number in primary hippocampal neurons at DIV14 and DIV21. (A) Primary hippocampal neurons (DIV14) were transfected with GFP (DIV12) and were treated with two different concentrations of BTA-EG6 (1 or 5 μM) or with vehicle (0.05% DMSO) for 24 h; after 24 h, spine densities were measured. (B) Spine number quantifications of A (vehicle: n = 21, 1 μM BTA-EG6: n = 24, 5 μM BTA-EG6: n = 18; **p < 0.01). (C) Primary hippocampal neurons (DIV21) were transfected with GFP (DIV19) and were treated with two different concentrations of BTA-EG6 (1 or 5 μM) or with vehicle (0.05% DMSO) for 24 h. (D) Quantification of data from C (vehicle: n = 44, 1 μM BTA-EG6: n = 22, 5 μM BTA-EG6: n = 17; ***p < 0.001). All values were expressed as mean ± SEM.
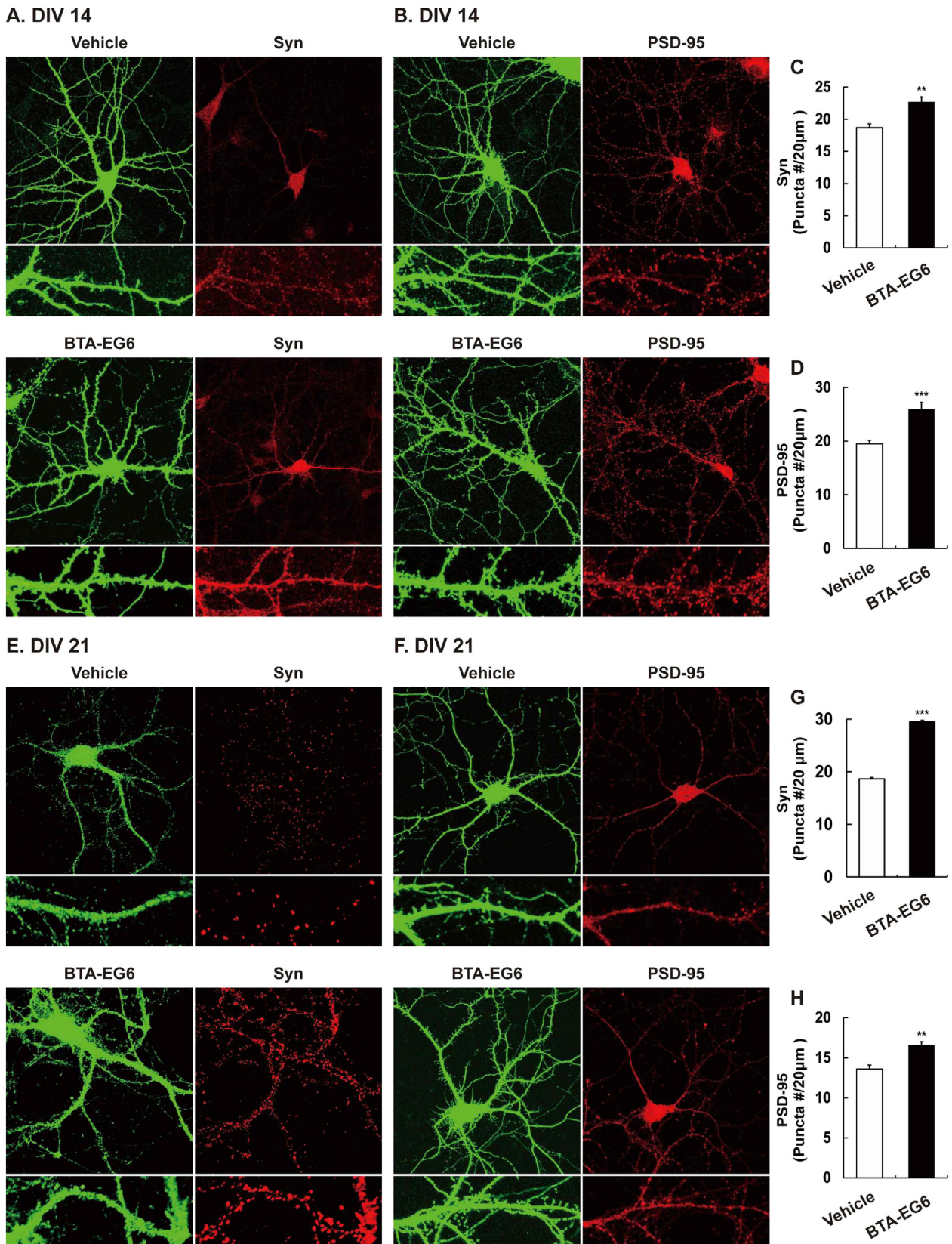
Fig. 2. BTA-EG6 increases puncta numbers of synaptophysin and PSD-95 in primary hippocampal neurons. (A–B) Primary hippocampal neurons (DIV14) were transfected with GFP and treated with BTA-EG6 (5 μM) or vehicle (0.05% DMSO) for 24 h. After 24 h, neurons were immunostained with synaptophysin (A) or PSD-95 (B) antibodies, respectively. (C–D) Quantification of data from A (vehicle: n = 6, BTA-EG6: n = 7; **p < 0.01) and B (vehicle: n = 4, BTA-EG6: n = 9; ***p < 0.001), respectively. (E–F) Primary hippocampal neurons (DIV21) were transfected with GFP and treated with 5 μM of BTA-EG6 or vehicle (0.05% DMSO) for 24 h. After 24 h of treatment, primary hippocampal cultures were immunostained with anti-synaptophysin (G, vehicle: n = 56, BTA-EG6: n = 62; ***p < 0.001) or anti-PSD-95 (H, vehicle: n = 5, BTA-EG6: n = 7; **p < 0.01), respectively. All values were expressed as mean ± SEM.

with brine, dried over sodium sulfate, and the solvent was removed under reduced pressure. The residue was purified via flash chromatography using 4% methanol in ethylacetate as the eluent to yield a yellow oil (isolated yield was 28%). ^{1}H-NMR (400 MHz, CD3OD): δ = 2.47 (s, 3 H), δ = 3.71–3.53 (m, 24 H), δ = 6.74 (d, 2 H, 8.4 Hz), δ = 7.29 (d, 2 H, 8.4 Hz), δ = 7.91–7.70 (m, 3 H). MS (ESI-positive): m/z 505.25 [MH$^+$] and 527.20 [MNa$^+$], calc. mass 504.23 [M$^+$].

2.2. Saturation shake-flask solubility method

To determine the difference in solubility between BTA-EG4 and BTA-EG6, a standard saturation shake-flask solubility method was performed with noted changes [17]. Briefly, ~5–10 mg of each compound was added into 5 mL of PBS (pH 7.4) and was shaken vigorously for 24 h at room temperature. After equilibrium was reached, the remaining un-dissolved compound was removed by centrifugation. The concentration of dissolved compound was then determined by measuring the UV–Vis absorbance at 355 nm (i.e., λ_{max} for both compounds). Dilutions in PBS were necessary for BTA-EG6 in order to obtain absorbance values under 1 absorbance unit, which facilitates precision in the measurement. No dilutions were necessary for BTA-EG4 due to its poor solubility in PBS. Concentrations were then determined by comparison to calibration curves for each respective compound. Data were presented as mean ± SD, n = 3.

2.3. Primary neuron culture, transfection and immunostaining

Primary hippocampal neurons (E19 Sprague–Dawley rats) were cultured at 150 cells/mm^2 as described previously [18]. To measure dendritic spine number, primary hippocampal neurons were transfected with green fluorescent protein (pEGFP, Clontech) and treated with BTA-EG6 or vehicle (0.05% DMSO) for 24 h, and dendritic spine number was measured. To measure the effects of BTA-EG6 on excitatory synapse number, primary hippocampal neurons were transfected with GFP and immunostained with anti-synaptophysin and anti-PSD-95.

Primary hippocampal neurons were transfected using Lipofectamine 2000 (Invitrogen, Carlsbad, CA, USA) with pEGFP and pLL3.7, pEGFP and RasGRF1 shRNA, pEGFP and HA vector or pEGFP and RasN17 and treated with BTA-EG6 (5 μM) or vehicle (0.05% DMSO) to determine the effect of BTA-EG6 on dendritic spine formation via Ras signaling dependent manner. RasGRF1-shRNA (5′-GCGCAATCTTCCGACTCAA-3′) was inserted into the pLL3.7 vector that simultaneously expresses RNAi-inducing shRNA and GFP under the U6 and CMV promoters, respectively [19,20]. The empty pLL3.7 vector was used as a negative control for the RasGRF1 shRNA.

After 24 h, we used the following antibodies: anti-GFP (Novus Biologicals), anti-GFP (Invitrogen), synaptophysin (Sigma), anti-PSD-95 (NeuroMabs, Davis, CA, USA), anti-GluA1 (Calbiochem), anti-GluA2 (BD Pharmagen), anti-GluN1 (Neuromab), anti-GluN2A (Neuromab), anti-GluN2B (Neuromab), anti-RasGRF1 (Santa Cruz; BD Biosciences), anti-p-ERK (Invitrogen), anti-ERK (Cell Signaling), anti-p-CREB (Millipore), anti-CREB (Cell Signaling), anti-CaMKIIα (Abcam), anti-CaMKIIβ (Abcam), anti-p-JNK (Cell signaling), anti-JNK (Cell signaling), anti-p38 (Cell signaling), anti-SPAR (generous gift from Daniel Pak at Georgetown University), anti-Cdc42 (Abcam), anti-PKC (Abcam), anti-CDK5 (Abcam), anti-Shank (Neuromab), and anti-SynCAM (Neuromab). Cultured primary hippocampal neurons were imaged using a LSM 510 laser scanning confocal microscope (Zeiss). Image analyses were performed using MetaMorph software to measure the average puncta number along the dendritic segments (Universal Imaging Corporation, Downington, PA, USA). We used Image J software to measure the average levels of proteins along the dendrite processes.

2.4. Cell surface biotinylation and Western blot

The cell surface biotinylation was conducted as previously described [21]. Briefly, cell surface proteins were biotinylated, isolated with avidin beads (Thermo Fischer Scientific, Waltham, MA, USA), and Western blotted. Total protein and Western blot were conducted as described previously [20]. We used the following antibodies: anti-GluA1, Anti-GluA2, anti-RasGRF1, anti-p-ERK(Invitrogen), anti-ERK (Cell Signaling), anti-p-CREB (Millipore), anti-CREB (Cell Signaling), anti-CaMKIIα (Abcam), anti-p-JNK (Cell signaling), anti-JNK (Cell signaling), and β-actin (Santa Cruz). Image analyses were performed using Image Gauge V4.0 and MetaMorph software to measure the average levels of band expression.

2.5. Image analyses

Quantification was performed blind and dendritic spines were defined according to standard morphological classification (protrusions 0.2–2 μm in length with or without a head and neck). Dendritic spine number was counted on secondary or tertiary dendritic branches using Scion Image software (Scion Corporation). Thresholding was performed at twice the background level and differences in GFP signal intensity were accounted for by selecting cells with similar levels of somatic GFP signal intensity (i.e. similar expression level). We excluded protrusions morphologically similar to filopodia. To measure the puncta numbers of synaptophysin and PSD-95, we examined secondary or tertiary dendritic segments (20 μm length beginning 10 μm from soma) and counted puncta using MetaMorph software (Molecular Devices). Measurement of puncta number was performed by manually counting and tracing each individual cluster along neuronal processes. Analysis and selection conditions were kept constant for all images within experiments.

2.6. Live cell surface immunostaining

To measure cell surface levels of GluA1 and GluA2, we conducted live cell surface staining [22]. Briefly, live primary hippocampal neurons were incubated with N-terminal recognized GluA1 or GluA2 antibodies (10 μg/mL in conditioned medium) for 10 min, and then fixed in 4% paraformaldehyde (non-permeabilizing conditions) for 5 min. After 5 min, primary hippocampal neurons were washed with 1× PBS for 3 times. After washing, Surface-labeled GluA1 or GluA2 were detected with Alexa fluor-555 (red color) secondary antibodies. Then the primary hippocampal cells were permeabilized in methanol (−20 °C, 90 s), and incubated with anti-GFP antibody.

2.7. Statistical analyses

All data analysis were performed using Graphpad Prism 5 software via either a 2-tailed t-test or ANOVA with Tukey's post-hoc test for multiple comparisons, with significance determined at p < 0.05.

3. Results

3.1. Development and synthesis of BTA-EG4 analog BTA-EG6

Solubility is an important parameter to achieve the desired concentrations of a drug in circulation for the anticipated pharmocological response. Unfortunately, BTA-EG4 has low solubility and can precipitate from solution, suggesting that it may not reach its target at a consistent and intended dose. To potentially optimize the potency of BTA-EG4, we synthesized and evaluated a BTA-EG4-analog with increased solubility in aqueous solution, BTA-EG6. To determine the difference in solubility between BTA-EG4 and BTA-EG6, we performed the saturation shake-flask solubility method [17]. We found that BTA-EG4 was visibly less soluble in PBS solution than BTA-EG6 (data not shown), and quantification revealed the solubility of BTA-EG6 was increased by two orders of magnitude over BTA-EG4 (Table 1).
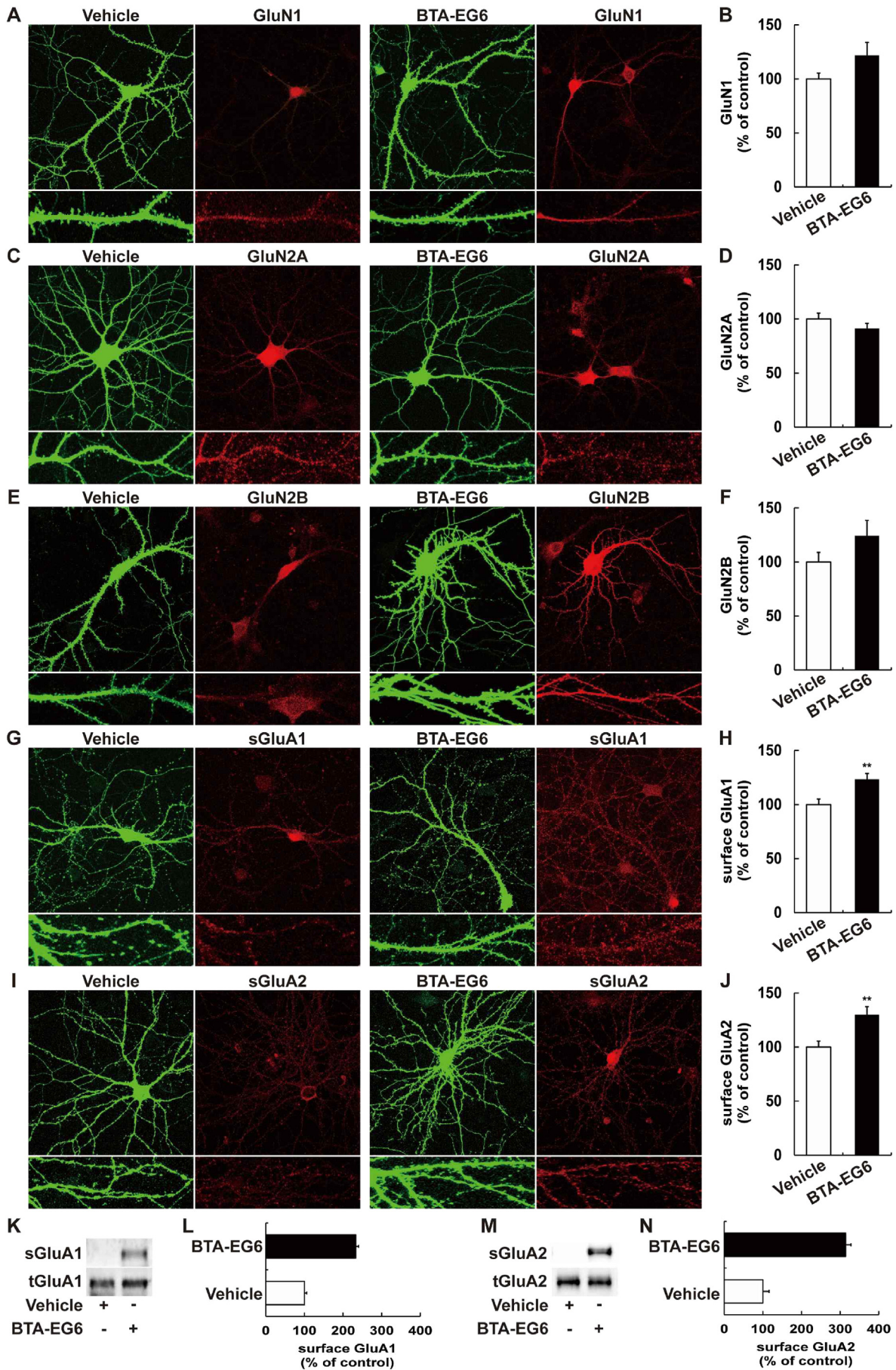
3.2. BTA-EG6 increases dendritic spine number in vitro

We have previously demonstrated that BTA-EG4 promotes dendritic spine formation [10,11]. To examine the effects of BTA-EG6 on dendritic spine formation, primary hippocampal neurons were transfected with GFP and treated with either BTA-EG6 (1 or 5 μM) or vehicle at day in vitro (DIV) 14 (which is the peak of synaptogenesis) and DIV21 (representing mature hippocampal neurons). After 24 h, spine densities were measured using Scion Image analysis. Interestingly, we found that 5 μM treatment of BTA-EG6 significantly increased dendritic spine number compared to both control and 1 μM treatment at DIV14 (Fig. 1A–B). Additionally, at DIV21, BTA-EG6 treatment significantly increased the dendritic spine number at both concentrations compared to the vehicle treatment (Fig. 1C–D). These results suggest that BTA-EG6 can increase dendritic spine number at both developmental and mature stages in primary hippocampal neurons.

3.3. BTA-EG6 increases the number of excitatory synapses in primary hippocampal neurons

To examine whether BTA-EG6 has an effect on excitatory synapse number, primary hippocampal neurons at DIV14 and DIV21 were transfected with GFP and treated with BTA-EG6 (5 μM) or vehicle for 24 h. After 24 h, cells were immunostained with synaptophysin (pre-synaptic marker) and PSD-95 (postsynaptic marker). We found that BTA-EG6-treated primary hippocampal neurons at DIV14 showed an increased puncta numbers of both synaptophysin and PSD-95 (Fig. 2A–D). Additionally, we observed that BTA-EG6-treated primary hippocampal neurons at DIV21 exhibited a significant increase in the puncta number of synaptophysin and PSD-95 (Fig. 2E–H). These results suggest that BTA-EG6 may promote synapse formation in primary hippocampal neurons.

3.4. BTA-EG6 increases the cell surface levels of GluA1 and GluA2

Our recent study has shown that BTA-EG4 increases the number of functional excitatory synapses [11], which consist of N-methyl-D-aspartate (NMDA) receptors and α-amino-3-hydroxy-5-methyl-4-isoxazolepropionic acid (AMPA) receptors [23,24]. To examine the effects of BTA-EG6 on the levels of NMDA receptor subunits GluN1, GluN2A, and GluN2B, primary hippocampal neurons were transfected with GFP (DIV19) and treated with either BTA-EG6 (5 μM) or vehicle for 24 h. After 24 h, we conducted immunostaining with GluN1, GluN2A, or GluN2B antibodies, and measured the total level of NMDA receptors using Scion Image analysis. We confirmed that the treatment with BTA-EG6 does not affect the expression level of GluN1, GluN2A, or GluN2B receptors compared to the treatment with the vehicle (Fig. 3A–F). Because the level of GluN1, GluN2A, or GluN2B receptors is shown no significant change by BTA-EG6, we did not confirm the cell surface level of NMDA receptors.

In contrast, after an identical treatment protocol, we conducted live cell surface immunostaining using N-terminal-recognized GluA1 or GluA2 antibodies, and measured the cell surface level of GluA1 or GluA2 receptors. We found that BTA-EG6 significantly increased the cell surface level of GluA1 and GluA2 receptors (Fig. 3G–J) assayed by live cell surface immunostaining. In addition, we conducted cell surface biotinylation by treating BTA-EG6 or vehicle in primary cortical neurons and found that BTA-EG6 increased cell surface levels of GluA1 and GluA2 (Fig. 3K–N). This result suggests that BTA-EG6 may affect AMPA receptor trafficking.

High surface levels of AMPA receptors have been shown to be able to induce dendritic spine growth [25]. Thus, our results further suggest that BTA-EG6 may improve spine growth. This is consistent with our previous findings with BTA-EG4, where it was implied that creating new synapses may be beneficial by allowing more synaptic contact points, not by enhancing long-term potentiation (LTP) at individual synapses [10].

3.5. BTA-EG6 increases spinogenesis through Ras signaling pathway

Upon establishing the foundation that BTA-EG6 increases dendritic spine formation, we further investigated into the molecular mechanism underlying this phenomenon. Ras is a well-studied GTPase that is known to be involved in neurodegenerative diseases as well as dendritic spine formation [26]. Furthermore, our recent work demonstrated that BTA-EG4 alters synapse formation via Ras signaling [10]. Thus, we hypothesized that the underpinning molecular mechanism of BTA-EG6's effects on dendritic spine formation involves Ras signaling.

To examine the involvement of Ras signaling in the effects of BTA-EG6, primary hippocampal neurons were transfected with GFP (DIV19), treated with BTA-EG6 (5 μM) or vehicle for 24 h, and immuno-stained for RasGRF1, a guanine nucleotide exchange factor involved in Ras activation. When treated with BTA-EG6, the level of RasGRF1 increased significantly compared to control (Fig. 4A–B). We also investigated whether BTA-EG6 alters p-ERK and p-CREB, downstream Ras signaling proteins. When treated with BTA-EG6, both p-ERK and p-CREB levels increased significantly, without altering the total ERK and CREB levels (Fig. 4C–J). As an alternative approach, we conducted Western blotting by treating with BTA-EG6 or control in primary cortical neurons and found that BTA-EG6 significantly increased the levels of RasGRF1 and p-ERK (Fig. 4K–N). We also found that BTA-EG6 produced a trend toward increased p-CREB, but did not alter the levels of ERK and CREB (Fig. 4M–P).

To further confirm that BTA-EG6's effect on dendritic spine formation is Ras-dependent, we conducted a RasGRF1 knockdown experiment by transfecting primary hippocampal neurons (DIV21) with GFP and RasGRF1 shRNA, or GFP and pLL3.7 (i.e., an empty vector control for shRNA). After 24 h, cells were treated with BTA-EG6 (5 μM) or vehicle, and dendritic spine number was measured. When treated with BTA-EG6, dendritic spine number was significantly increased compared to vehicle treatment (Fig. 5A–B). Knockdown of RasGRF1 by itself significantly decreased dendritic spine number. Importantly, BTA-EG6 treatment failed to enhance dendritic spine number in the absence of RasGRF1 (Fig. 5A–B).

Additionally, we found that overexpression of dominant negative mutant RasN17 prevented the effects of BTA-EG6 on dendritic spine formation (Fig. 5C–D). These results demonstrate that the underlying mechanism of BTA-EG6 in increasing dendritic spine number is Ras pathway dependent.

3.6. BTA-EG6 increased the puncta density of CaMKIIa

Previous studies have demonstrated that CaMKII is implicated in dendritic spine formation and NMDA receptor signaling [27] as well as

---

Fig. 3. BTA-EG6 increases the cell surface levels of AMPA receptor subunits. (A, C, E) Primary hippocampal neurons at DIV19 were transfected with GFP and treated with BTA-EG6 (5 μM) or vehicle (0.05% DMSO) for 24 h. After 24 h, immunostaining was conducted with anti-GluN1, anti-GluN2A, and anti-GluN2B, respectively, and their total levels were measured. (B, D, F) Quantification of data from A (vehicle: n = 13, BTA-EG6: n = 15), C (vehicle: n = 11, BTA-EG6: n = 8), and E (vehicle: n = 5, BTA-EG6: n = 8), respectively. (G, I) Primary hippocampal neurons were transfected with GFP at DIV19 and treated with BTA-EG6 (5 μM) or vehicle (0.05% DMSO) for 24 h. After 24 h of treatment, live cell surface immunostaining was conducted with N-terminal recognizing GluA1 and GluA2 antibodies, respectively, and their surface levels were measured. (H, J). (K, M) Primary cortical neurons were treated with BTA-EG6 (5 μM) or vehicle (0.05% DMSO) for 24 h. After 24 h of treatment, cell surface biotinalytion was conducted and their surface levels were measured. (L, N) Quantification of data from L (vehicle: n = 2, BTA-EG6: n = 2) and N (vehicle: n = 3, BTA-EG6: n = 3). All values were expressed as mean ± SEM.
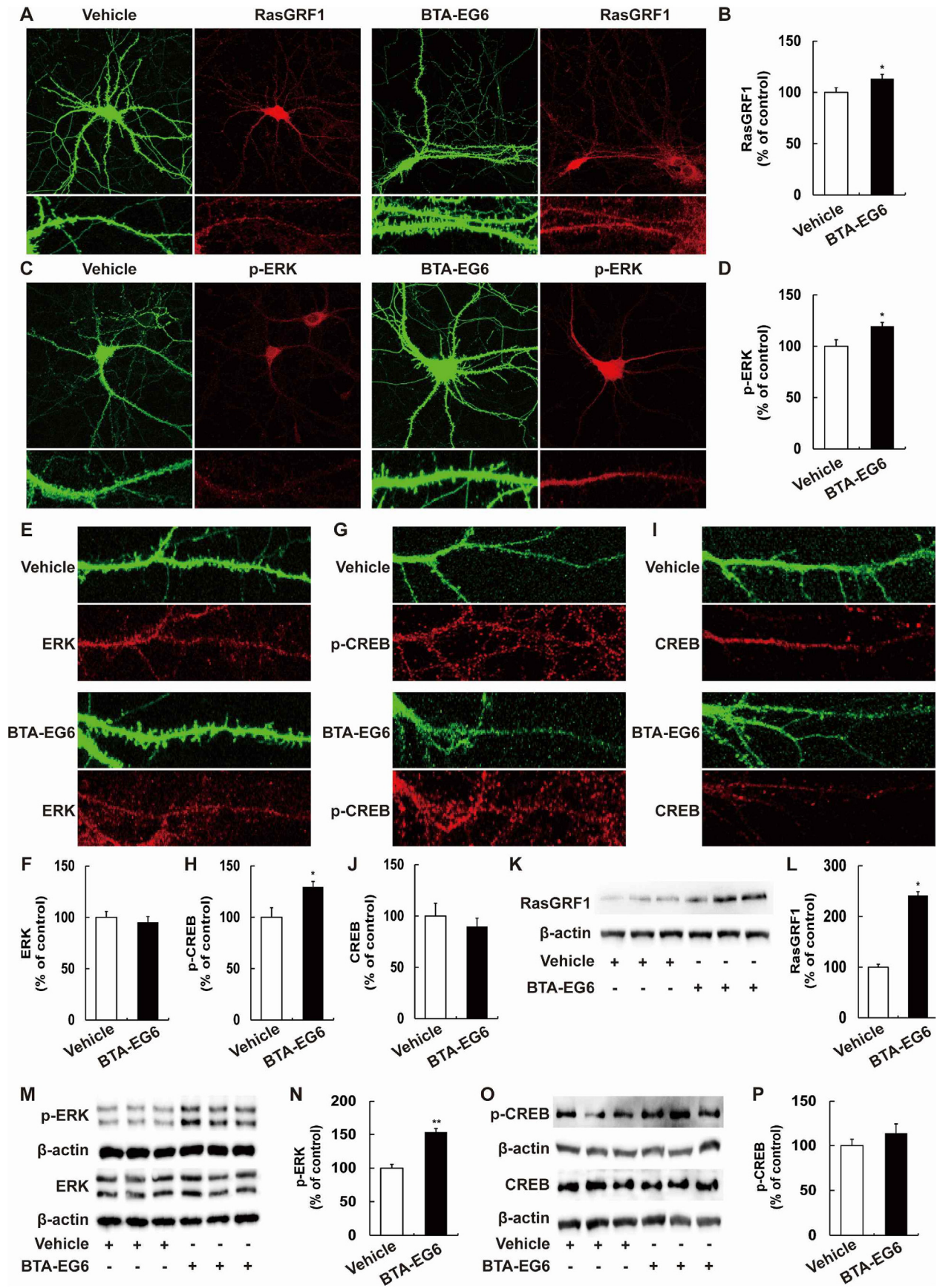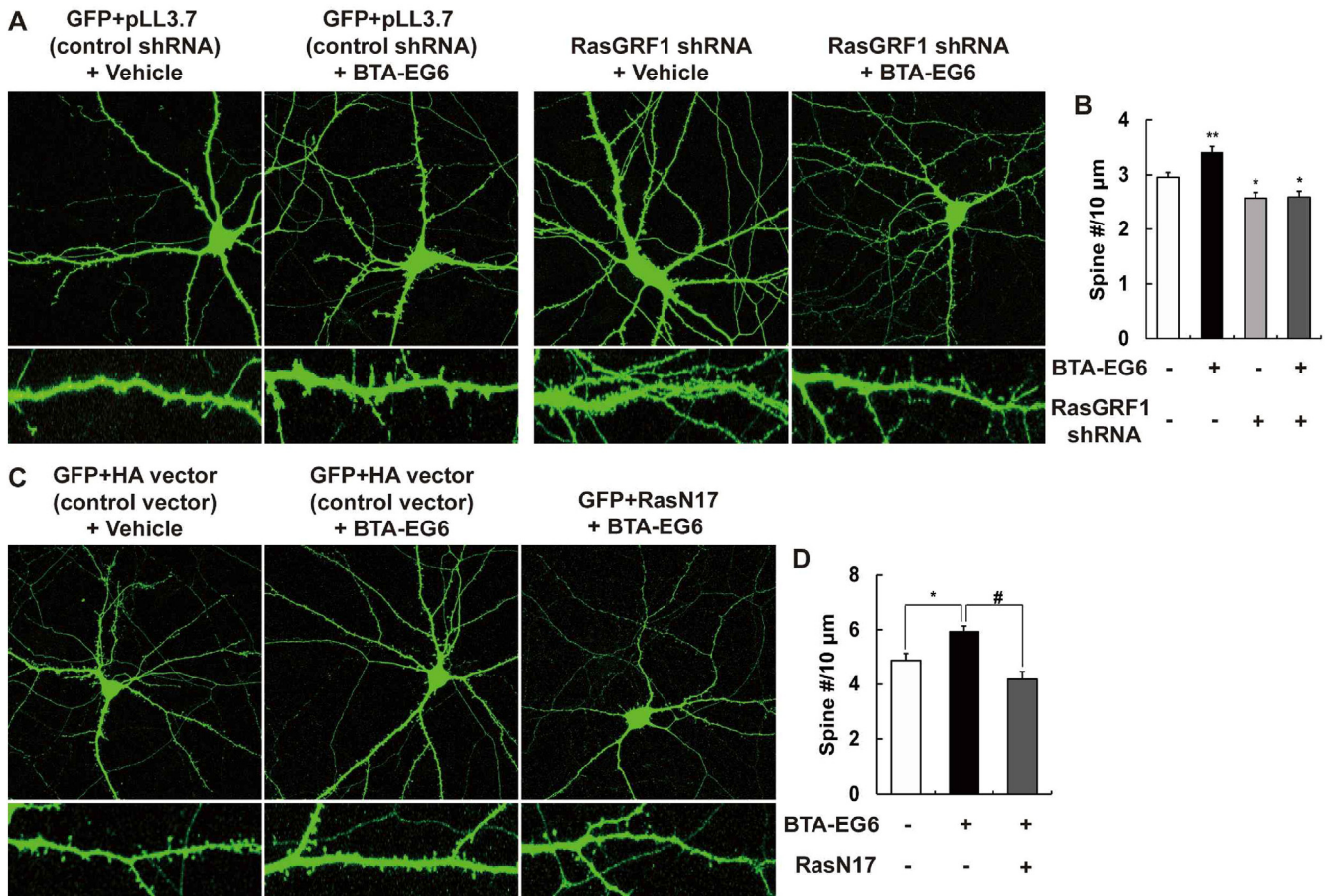
Fig. 5. Enhanced dendritic spinogenesis by BTA-EG6 depends on Ras signaling pathway. (A) Primary hippocampal neurons were transfected with GFP and pLL3.7 or with GFP and RasGRF1 shRNA; the cultures were then treated with vehicle (0.05% DMSO) or BTA-EG6 (5 μM) for 24 h. Afterwards, dendritic spine densities were measured and quantified. (B) Quantification of data from A (GFP + pLL3.7 with vehicle: n = 31, GFP + pLL3.7 with BTA-EG6: n = 31, GFP + RasGRF1 shRNA with vehicle: n = 22, GFP + RasGRF1 shRNA with BTA-EG6: n = 21; *p < 0.05, **p < 0.01). (C) Primary hippocampal neurons were transfected with GFP and HA vector or with GFP and RasN17; the cultures were then treated with BTA-EG6 (5 μM) or vehicle (0.05% DMSO). Afterwards, dendritic spine densities were measured and quantified. (D) Quantification of data from C (GFP + HA with vehicle: n = 17, GFP + HA with BTA-EG6: n = 34, GFP + RasN17 with BTA-EG6: n = 21; *p < 0.05, #p < 0.05 vs. BTA-EG6). All values were expressed as mean ± SEM.

long-term memory in AD mouse models [28]. We initially examined whether BTA-EG6 affected the levels of CaMKIIα and CaMKIIβ. For this experiment, primary hippocampal neurons were transfected with GFP (DIV19), and treated with BTA-EG6 (5 μM) or vehicle for 24 h. We then conducted immunostaining with CaMKIIα antibody and found that BTA-EG6 significantly increased the puncta density of CaMKIIα (Fig. 6A–B). In addition, we found that BTA-EG6 treated primary cortical neurons significantly increased the levels of CaMKIIα (Fig. 6C–D) by Western blotting. However, BTA-EG6 did not alter the puncta density of CaMKIIβ (Fig. 6E–F). These results suggest that BTA-EG6 effects may involve CaMKIIα to alter spinogenesis.

3.7. BTA-EG6 does not affect the Rap signaling pathway

Previous studies have shown that defects in Rap signaling may be related to neurodegenerative diseases such as AD by stimulating the synaptic removal of AMPA receptors [29–31]. To investigate whether the molecular mechanism of BTA-EG6 is also Rap-dependent, primary hippocampal neurons (DIV21) were transfected with GFP (DIV19), and

treated with BTA-EG6 (5 μM) or vehicle for 24 h. After 24 h, we conducted immunostaining with antibodies for the downstream products of Rap signaling pathway, including phosphorylation of c-Jun. N terminal kinases (JNK) (Fig. 7A–B), JNK (Fig. 7C–D), spine-associated Rap guanosine triphosphatase-activating protein (SPAR) (Fig. 7E–F), and p38 (Fig. 7G–H), and measured their levels of expression. We also conducted Western blotting by treating with BTA-EG6 or vehicle in primary cortical neurons and confirmed that BTA-EG6 did not alter the protein levels of p-JNK and JNK (Fig.7I–K). The results showed that none of the downstream proteins of Rap signaling pathway was affected by BTA-EG6 (Fig. 7A–K). This result suggests that the BTA-EG6 may not affect the expression of Rap and or the downstream signaling pathway of Rap.

3.8. BTA-EG6 alters the levels of Cdc42, CDK5, and Shank

We examined whether BTA-EG6 can alter the levels of other spinogenesis-related proteins. For this experiment, primary hippocampal neurons were transfected with GFP (DIV19), and treated with BTA-EG6 (5 μM) or vehicle for 24 h. After 24 h, we conducted immunostaining

Fig. 4. BTA-EG6 increases the levels of Ras signaling pathway proteins in primary hippocampal neurons. (A, C, E, G, I) Primary hippocampal neurons were transfected with GFP at DIV19, treated with BTA-EG6 (5 μM) or vehicle for 24 h, and immunostained with antibodies of RasGRF1, p-ERK, ERK, p-CREB, and CREB, respectively; afterwards, protein intensities were measured and quantified. (B, D, F, H, J) Quantification of data from A (vehicle: n = 14, BTA-EG6: n = 15; *p < 0.05), C (vehicle: n = 6, BTA-EG6: n = 7; *p < 0.05), E (vehicle: n = 11, BTA-EG6: n = 13), G (vehicle: n = 5, BTA-EG6: n = 6; *p < 0.05), and I (vehicle: n = 7, BTA-EG6: n = 8), respectively. (K, M, O) Primary cortical neurons were treated with BTA-EG6 (5 μM) or vehicle (0.05% DMSO) for 24 h. After 24 h of treatment, Western blotting was conducted with RasGRF1, p-ERK, ERK, p-CREB, CREB, and β-actin. (L, N, P) Quantification of data from K (vehicle: n = 3, BTA-EG6: n = 3), M (vehicle: n = 9, BTA-EG6: n = 9), and O (vehicle: n = 3, BTA-EG6 n = 3). All values were expressed as mean ± SEM.
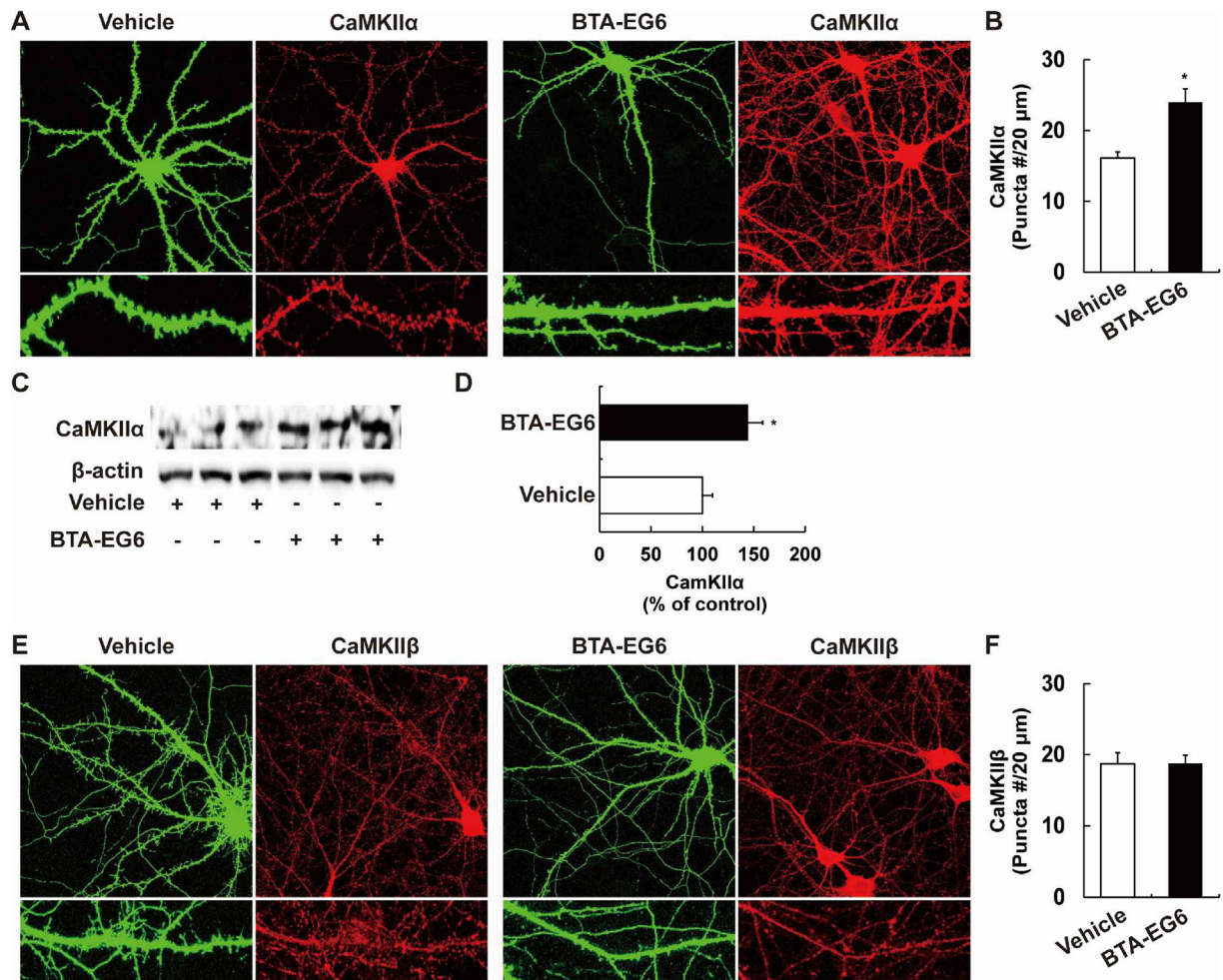
Fig. 6. BTA-EG6 increases the puncta number of CaMKIIα but not of CaMKIIβ. (A, E) Primary hippocampal neurons were transfected with GFP at DIV19, treated with BTA-EG6 (5 μM) or vehicle (0.05% DMSO) for 24 h and immunostained with CaMKIIα or CaMKIIβ antibodies. Analyses for the protein intensity and puncta numbers were performed thereafter. (B, F) Quantification of puncta number analyses performed for A (vehicle: n = 7, BTA-EG6: n = 4; *p < 0.05) and E (vehicle: n = 7, BTA-EG6: n = 8), respectively. (C) Primary cortical neurons were treated with BTA-EG6 (5 μM) or vehicle (0.05% DMSO) for 24 h. After 24 h of treatment, Western blotting was conducted with CaMKIIα and β-actin. (D) Quantification of data from C (vehicle: n = 3, BTA-EG6: n = 3). All values were expressed as mean ± SEM.

with cell division control protein (Cdc42), protein kinase C (PKC), cyclin-dependent kinase (CDK5), Shank, or SynCAM antibodies, and measured their levels of expression. The results show that treatment with BTA-EG6 significantly increases the levels of Cdc42 (Fig. 8A–B), CDK5 (Fig. 8C–D), and Shank (Fig. 8G–H). However, BTA-EG6 treatment did not affect PKC (Fig. 8E–F) and SynCAM levels (Fig. 8I–J). These data suggest that BTA-EG6 alters spinogenesis with a potential involvement of Cdc42, CDK5, and Shank.

4. Discussion

We have previously demonstrated that BTA-EG4 increases dendritic spine number via Ras-mediated signaling, and that BTA-EG4-injected wild-type mice have higher dendritic spine number with increased puncta number of synaptophysin and PSD-95 [10]. In the present study, we have examined the spinogenic activity of BTA-EG6, an analog of BTA-EG4 with an increased solubility in aqueous solutions. Using primary hippocampal neurons, we found that BTA-EG6 can significantly promote dendritic spine formation at the peak of synaptogenesis (DIV14) as well as in mature neurons (DIV21). We also found that BTA-EG6 significantly increases the puncta densities of synaptophysin and PSD-95 more effectively during development compared to after maturation; this finding suggests that BTA-EG6 may affect functional synapses. Moreover, our results suggest that BTA-EG6 promotes spinogenesis through RasGRF1-Ras signaling pathway.

Additionally, we previously established that BTA-EG4-injected wild-type mice do not show a change in either total or surface level of NMDA or AMPA receptor subunits [10]. However, in the present study, BTA-EG6 increased the cell surface level of AMPA receptors in vitro. This difference in the effects of BTA-EG4 and BTA-EG6 on the levels of AMPA receptors is interesting. This discrepancy may be due to the fact that BTA-EG6 experiments conducted here were primarily in vitro and BTA-EG6 has more hydrophilic character than BTA-EG4 [12].

In order to investigate into the molecular mechanism of BTA-EG6, we examined whether a Ras signaling pathway would be involved; a Ras signaling cascade was previously shown to be altered upon BTA-EG4 treatment [10]. Here, we found that BTA-EG6 affects the level of Ras signaling proteins and alters spine number in a Ras-dependent manner. Further, we examined whether BTA-EG6 can alter the downstream molecules of the Ras signaling cascade, such as CaMKIIα and CaMKIIβ [32,33]. Interestingly, we found that BTA-EG6 significantly alters the puncta number of CaMKIIα, but not of CaMKIIβ, suggesting that BTA-EG6 may selectively recruit CaMKIIα to promote spinogenesis.

We then investigated whether BTA-EG6 involves other signaling pathways to affect dendritic spine number. Therefore, we analyzed the effects of BTA-EG6 on Rap signaling proteins, which are known to be implicated in dendritic spine retardation. In addition, a Rap effector, JNK, was previously shown to be involved in AD, where AD patients have increased JNK activity [34,35]. Similarly, p38 has been shown to be associated with increased amyloid deposition in AD mouse models [36].
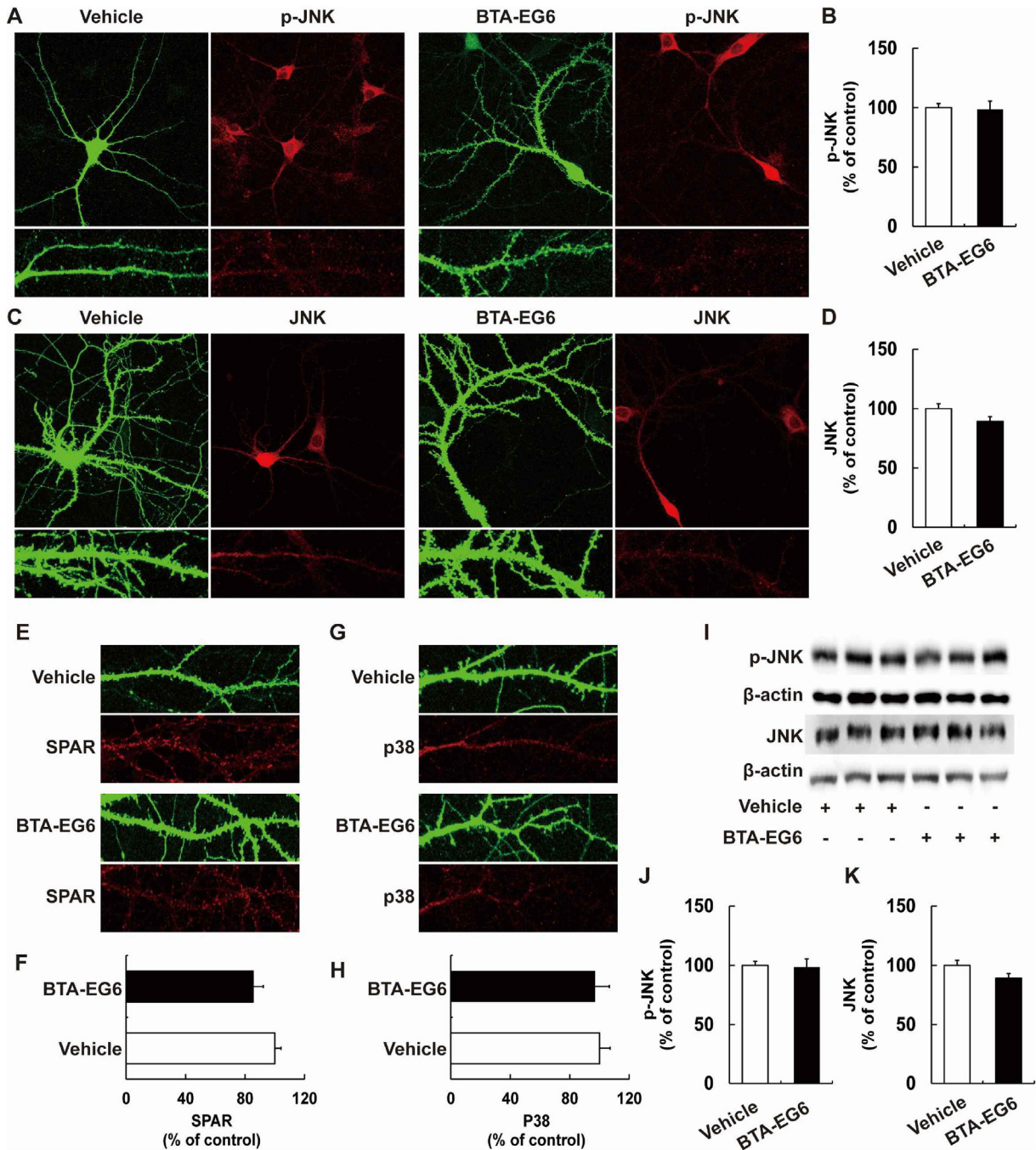
Fig. 7. BTA-EG6 does not alter downstream proteins of Rap signaling pathway. (A, C, E, G) Primary hippocampal neurons were transfected with GFP at DIV19 and then treated with BTA-EG6 (5 μM) or vehicle (0.05% DMSO) for 24 h. After 24 h, neurons were immunostained with the antibodies for p-JNK, JNK, SPAR, and p38, respectively. (B, D, F, H) Quantification of data from A (vehicle: n = 13, BTA-EG6: n = 19), C (vehicle: n = 6, BTA-EG6: n = 7), E (vehicle: n = 5, BTA-EG6: n = 10), and G (vehicle: n = 7, BTA-EG6: n = 14), respectively. (I) Primary cortical neurons were treated with BTA-EG6 (5 μM) or vehicle (0.05% DMSO) for 24 h. After 24 h of treatment, Western blotting was conducted with p-JNK, JNK, and β-actin. (J, K) Quantification of data from I (vehicle: n = 9, BTA-EG6: n = 9). All values were expressed as mean ± SEM.

Furthermore, SPAR, one of the PSD proteins that interact with PSD-95, has been suggested to function as a spine regulator [18]. Upon investigation into these Rap signaling proteins, we found that BTA-EG6 does not affect the levels of Rap signaling molecules, including p-JNK, p38, and SPAR. These results suggest that BTA-EG6 regulates dendritic spine formation possibly via a Rap-independent mechanism.

Upon establishing the specific involvement of Ras signaling cascade, we furthered our investigation to elucidate other target proteins on which BTA-EG6 exerts its effects. We hypothesized that BTA-EG6 would require other spinogenesis-related proteins to promote spinogenesis. To test this hypothesis, we examined the levels of CDK5,

which has been shown to be associated with the risk of AD [37], and the hyperactivity of which results in the production of Aβ aggregates [38]. We also looked into Cdc42, which plays an important role in neuronal morphology [39]. Interestingly, we observed that BTA-EG6 significantly affects the level of these two proteins, suggesting that BTA-EG6 may regulate the distribution pattern and expression levels of CDK5 and Cdc42 to affect dendritic spine number.

The mechanism through which BTA-EG6 regulates Ras signaling proteins as well as other spinogenesis-related proteins has not yet been firmly established. One possible explanation involves the interaction between Aβ aggregates and the Ras signaling pathway. It has
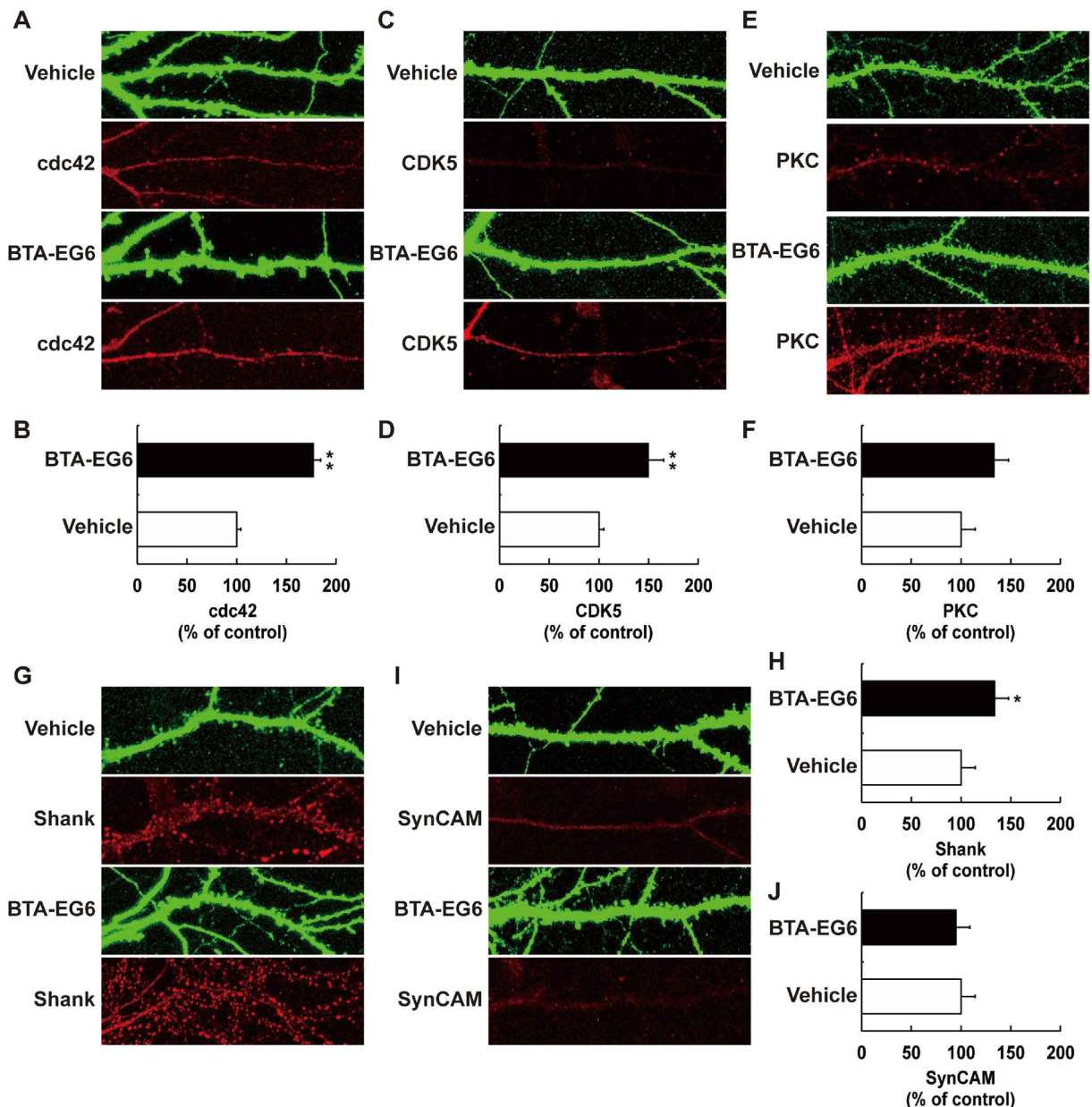
Fig. 8. BTA-EG6 alters the levels of CDC42 and CDK5. (A, C, E, G, I) Primary hippocampal neurons were transfected with GFP at DIV19, treated with BTA-EG6 (5 μM) or vehicle (0.05% DMSO) for 24 h, and immunostained with antibodies for Cdc42, PKC, CDK5, Shank, and SynCAM, respectively. Protein intensities were measured and quantified afterwards. (B, D, F, H, J) Quantification of data from A (vehicle: n = 7, BTA-EG6: n = 14; **p < 0.01), C (vehicle: n = 7, BTA-EG6: n = 11; **p < 0.01), E (vehicle: n = 10, BTA-EG6: n = 13), G (vehicle: n = 8, BTA-EG6: n = 12; **p < 0.05), and I (vehicle: n = 7, BTA-EG6: n = 12), respectively. All values were expressed as mean ± SEM.

been reported that Aβ inhibits the activity of Ras to regulate spinogenesis [40]. BTA-EG6 may bind Aβ and neutralize Aβ toxicity and, in turn, block the effects of Aβ on Ras activity to alter spinogenesis as well as synaptic function. Future studies using an AD model mouse may help examine the effect of amyloid-β on the spinogenic effects of BTA-EG6. Another possible explanation revolves around the possibility that BTA-EG6 may bind amyloid precursor protein (APP) and affect dendritic spine formation. Lastly, it is still unclear whether the interaction between BTA-EG6 and Cdc42 and CDK5 alters dendritic spine density directly or indirectly. Here, we have mainly focused on the effects of BTA-EG6 on dendritic spine formation and its underlying molecular mechanism using in vitro systems. Further in-depth studies with experiments in vivo are in progress in order to examine the differences

between the effects and efficacy of BTA-EG4 and BTA-EG6 and to clearly elucidate the underpinning molecular mechanism.

Together, our results are the first to demonstrate that a BTA-EG4 analog, BTA-EG6, significantly increases spinogenesis through a RasGRF1-ERK signaling pathway with potential involvement of CaMKIIα, Cdc42, and CDK5. Overall, our results shed light on another promising compound for enhancing neuronal and synaptic function in the normal brain and reveals potential therapeutic applications for AD.

Conflict of interest

None declared.

Transparency document

The Transparency document associated with this article can be found, in the online version.

Acknowledgments

References

[1] D.M. Holtzman, E. Mandelkow, D.J. Selkoe, Alzheimer disease in 2020, Cold Spring Harb. Perspect Med. 2 (2012).

[2] D.J. Selkoe, SnapShot: pathobiology of Alzheimer's disease, Cell 154 (2013) 468 e461.

[3] D.J. Selkoe, Altered structural proteins in plaques and tangles: what do they tell us about the biology of Alzheimer's disease? Neurobiol. Aging 7 (1986) 425–432.

[4] S. Wei, S.L. Soh, W. Qiu, W. Yang, C.J. Seah, J. Guo, W.Y. Ong, Z.P. Pang, W. Han, Seipin regulates excitatory synaptic transmission in cortical neurons, J. Neurochem. 124 (2013) 478–489.

[5] A. Alpar, U. Ueberham, M.K. Bruckner, G. Seeger, T. Arendt, U. Gartner, Different dendrite and dendritic spine alterations in basal and apical arbors in mutant human amyloid precursor protein transgenic mice, Brain Res. 1099 (2006) 189–198.

[6] D.M. Walsh, D.J. Selkoe, Deciphering the molecular basis of memory failure in Alzheimer's disease, Neuron 44 (2004) 181–193.

[7] M.A. Chabrier, D. Cheng, N.A. Castello, K.N. Green, F.M. LaFerla, Synergistic effects of amyloid-beta and wild-type human tau on dendritic spine loss in a floxed double transgenic model of Alzheimer's disease, Neurobiol. Dis. 64 (2014) 107–117.

[8] A.M. Pooler, W. Noble, D.P. Hanger, A role for tau at the synapse in Alzheimer's disease pathogenesis, Neuropharmacology 76 Pt A (2014) 1–8.

[9] A. Kremer, H. Maurin, D. Demedts, H. Devijver, P. Borghgraef, F. Van Leuven, Early improved and late defective cognition is reflected by dendritic spines in Tau.P301L mice, J. Neurosci. 31 (2011) 18036–18047.

[10] A. Megill, T. Lee, A.M. DiBattista, J.M. Song, M.H. Spitzer, M. Rubinshtein, L.K. Habib, C.C. Capule, M. Mayer, R.S. Turner, A. Kirkwood, J. Yang, D.T. Pak, H.K. Lee, H.S. Hoe, A tetra(ethylene glycol) derivative of benzothiazole aniline enhances Ras-mediated spinogenesis, J. Neurosci. 33 (2013) 9306–9318.

[11] J.M. Song, A.M. DiBattista, Y.M. Sung, J.M. Ahn, R.S. Turner, J. Yang, D.T. Pak, H.K. Lee, H.S. Hoe, A tetra(ethylene glycol) derivative of benzothiazole aniline ameliorates dendritic spine density and cognitive function in a mouse model of Alzheimer's disease, Exp. Neurol. 252 (2014) 105–113.

[12] P. Inbar, C.Q. Li, S.A. Takayama, M.R. Bautista, J. Yang, Oligo(ethylene glycol) derivatives of thioflavin T as inhibitors of protein–amyloid interactions, Chembiochem 7 (2006) 1563–1566.

[13] J.S. Olsen, C. Brown, C.C. Capule, M. Rubinshtein, T.M. Doran, R.K. Srivastava, C. Feng, B.L. Nilsson, J. Yang, S. Dewhurst, Amyloid-binding small molecules efficiently block SEVI (semen-derived enhancer of virus infection)- and semen-mediated enhancement of HIV-1 infection, J. Biol. Chem. 285 (2010) 35488–35496.

[14] D.A. Sheik, L. Brooks, K. Frantzen, S. Dewhurst, J. Yang, Inhibition of the enhancement of infection of human immunodeficiency virus by semen-derived enhancer of virus infection using amyloid-targeting polymeric nanoparticles, ACS Nano 9 (2015) 1829–1836.

[15] P. Inbar, J. Yang, Inhibiting protein–amyloid interactions with small molecules: a surface chemistry approach, Bioorg. Med. Chem. Lett. 16 (2006) 1076–1079.

[16] L.K. Habib, M.T. Lee, J. Yang, Inhibitors of catalase–amyloid interactions protect cells from beta-amyloid-induced oxidative stress and toxicity, J. Biol. Chem. 285 (2010) 38933–38943.

[17] E. Baka, J.E. Comer, K. Takacs-Novak, Study of equilibrium solubility measurement by saturation shake-flask method using hydrochlorothiazide as model compound, J. Pharm. Biomed. Anal. 46 (2008) 335–341.

[18] D.T. Pak, S. Yang, S. Rudolph-Correia, E. Kim, M. Sheng, Regulation of dendritic spine morphology by SPAR, a PSD-95-associated RapGAP, Neuron 31 (2001) 289–303.

[19] D.A. Rubinson, C.P. Dillon, A.V. Kwiatkowski, C. Sievers, L. Yang, J. Kopinja, D.L. Rooney, M. Zhang, M.M. Ihrig, M.T. McManus, F.B. Gertler, M.L. Scott, L. Van Parijs, A lentivirus-based system to functionally silence genes in primary mammalian cells, stem cells and transgenic mice by RNA interference, Nat. Genet. 33 (2003) 401–406.

[20] K.J. Lee, Y. Lee, A. Rozeboom, J.Y. Lee, N. Udagawa, H.S. Hoe, D.T. Pak, Requirement for Plk2 in orchestrated ras and rap signaling, homeostatic structural plasticity, and memory, Neuron 69 (2011) 957–973.

[21] S.B. Dumanis, H.J. Cha, J.M. Song, J.H. Trotter, M. Spitzer, J.Y. Lee, E.J. Weeber, R.S. Turner, D.T. Pak, G.W. Rebeck, H.S. Hoe, ApoE receptor 2 regulates synapse and dendritic spine formation, PLoS One 6 (2011), e17203.

[22] Y.I. Sohn, N.J. Lee, A. Chung, J.M. Saavedra, R. Scott Turner, D.T. Pak, H.S. Hoe, Antihypertensive drug Valsartan promotes dendritic spine density by altering AMPA receptor trafficking, Biochem. Biophys. Res. Commun. 439 (2013) 464–470.

[23] R.G. Morris, NMDA receptors and memory encoding, Neuropharmacology 74 (2013) 32–40.

[24] G. Wang, J. Gilbert, H.Y. Man, AMPA receptor trafficking in homeostatic synaptic plasticity: functional molecules and signaling cascades, Neural. Plast. 2012 (2012) 825364.

[25] M.I. Hamad, Z.L. Ma-Hogemeier, C. Riedel, C. Conrads, T. Veitinger, T. Habijan, J.N. Schulz, M. Krause, M.J. Wirth, M. Hollmann, P. Wahle, Cell class-specific regulation of neocortical dendrite and spine growth by AMPA receptor splice and editing variants, Development 138 (2011) 4301–4313.

[26] J. Zhu, G.F. Cao, Y.H. Dang, T. Chen, Structural plasticity associated with drugs addiction, Sheng Li Ke Xue Jin Zhan 42 (2011) 413–418.

[27] B. Bingol, C.F. Wang, D. Arnott, D. Cheng, J. Peng, M. Sheng, Autophosphorylated CaMKIIalpha acts as a scaffold to recruit proteasomes to dendritic spines, Cell 140 (2010) 567–578.

[28] D.M. Wang, Y.J. Yang, L. Zhang, X. Zhang, F.F. Guan, L.F. Zhang, Naringin enhances CaMKII activity and improves long-term memory in a mouse model of Alzheimer's disease, Int. J. Mol. Sci. 14 (2013) 5576–5586.

[29] R.L. Stornetta, J.J. Zhu, Ras and Rap signaling in synaptic plasticity and mental disorders, Neuroscientist 17 (2011) 54–78.

[30] J.J. Zhu, Y. Qin, M. Zhao, L. Van Aelst, R. Malinow, Ras and Rap control AMPA receptor trafficking during synaptic plasticity, Cell 110 (2002) 443–455.

[31] Y. Zhu, D. Pak, Y. Qin, S.G. McCormack, M.J. Kim, J.P. Baumgart, V. Velamoor, Y.P. Auberson, P. Osten, L. van Aelst, M. Sheng, J.J. Zhu, Rap2-JNK removes synaptic AMPA receptors during depotentiation, Neuron 46 (2005) 905–916.

[32] S.J. Lee, R. Yasuda, Spatiotemporal regulation of signaling in and out of dendritic spines: CaMKII and Ras, Open Neurosci. J. 3 (2009) 117–127.

[33] M. Salzano, M.R. Rusciano, E. Russo, M. Bifulco, L. Postiglione, M. Vitale, Calcium/calmodulin-dependent protein kinase II (CaMKII) phosphorylates Raf-1 at serine 338 and mediates Ras-stimulated Raf-1 activation, Cell Cycle 11 (2012) 2100–2106.

[34] A. Sclip, A. Arnaboldi, I. Colombo, P. Veglianese, L. Colombo, M. Messa, S. Mancini, S. Cimini, F. Morelli, X. Antoniou, E. Welker, M. Salmona, T. Borsello, Soluble Abeta oligomer-induced synaptopathy: c-Jun N-terminal kinases role, J. Mol. Cell Biol. 5 (2013) 277–279.

[35] A. Sclip, A. Tozzi, A. Abaza, D. Cardinetti, I. Colombo, P. Calabresi, M. Salmona, E. Welker, T. Borsello, c-Jun N-terminal kinase has a key role in Alzheimer disease synaptic dysfunction in vivo, Cell Death Dis. 5 (2014) e1019.

[36] M.J. Savage, Y.G. Lin, J.R. Ciallella, D.G. Flood, R.W. Scott, Activation of c-Jun N-terminal kinase and p38 in an Alzheimer's disease model is associated with amyloid deposition, J. Neurosci. 22 (2002) 3376–3385.

[37] G.A. Czapski, A. Maruszak, M. Styczynska, C. Zekanowski, K. Safranow, J.B. Strosznajder, Association between plasma biomarkers, CDK5 polymorphism and the risk of Alzheimer's disease, Acta Neurobiol. Exp. (Wars) 72 (2012) 397–411.

[38] V. Shukla, V. Skuntz, H.C. Pant, Deregulated Cdk5 activity is involved in inducing Alzheimer's disease, Arch. Med. Res. 43 (2012) 655–662.

[39] C. Chen, A. Wirth, E. Ponimaskin, Cdc42: an important regulator of neuronal morphology, Int. J. Biochem. Cell Biol. 44 (2012) 447–451.

[40] E.M. Szatmari, A.F. Oliveira, E.J. Sumner, R. Yasuda, Centaurin-alpha1-Ras-Elk-1 signaling at mitochondria mediates beta-amyloid-induced synaptic dysfunction, J. Neurosci. 33 (2013) 5367–5374.